Ecological Engineering 119 (2018) 73–83

Contents lists available at ScienceDirect

Ecological Engineering

journal homepage: www.elsevier.com/locate/ecoleng

New methodology of evaluation of best management practices performances for an agricultural watershed according to the climate change scenarios: A hybrid use of deterministic and decision support models

Dong Jin Jeon[a], Seo Jin Ki[b], YoonKyung Cha[c], Yongeun Park[d], Joon Ha Kim[a,*]

[a] School of Environmental Science and Engineering, Gwangju Institute of Science and Technology (GIST), 123 Cheomdangwagi-ro, Buk-gu, Gwangju 61005, Republic of Korea
[b] Department of Environmental Engineering, Gyeongnam National University of Science and Technology, 33 Dongjin-ro, Jinju-si, Gyeongsangnam-do 52725, Republic of Korea
[c] Department of Environmental Engineering, University of Seoul, 163 Seoulsiripdaero, Dongdaemun-gu, Seoul 02504, Republic of Korea
[d] School of Civil and Environmental Engineering, Konkuk University, 120 Neungdong-ro, Gwangjin-gu, Seoul 05029, Republic of Korea

ARTICLE INFO

Keywords:
Climate change
Best management practices
SWAT
Diffuse pollution
Multi-objective optimization

ABSTRACT

Climate change is a primary driver that alters water pollution hotspots in watersheds, which complicates the use of Best management practices (BMPs) for diffuse pollution mitigation strategies. The objective of this study is to evaluate future changes in BMPs on total phosphorus (TP) loads to the river system, depending on climate change. Current weather data were collected from 2000 to 2010 and future weather data from 2040 to 2050 were obtained from regional climate model simulations based on Representative Concentration Pathways (RCP) 2.6, 4.5, and 8.5 scenarios. This study describes various BMP implementation plans at affordable cost that are adapted to different weather conditions, current (for 2000–2010) and future climate scenarios (for 2040–2050). The Soil and Water Assessment Tool (SWAT), i.e., one of the deterministic models for watershed management, was used to estimate total phosphorus (TP) removal efficiency of various types of BMP at two crop fields (rice paddy and soybean fields) in the Yeongsan River (YR) watershed of Korea. The Non-dominated Sorting Genetic Algorithm II (NSGA-II), i.e., one of the artificial intelligence (AI) models for decision support framework, was applied to obtain allow for trade-off analysis between two conflict objectives, the maximum TP load reduction against implementation costs. The SWAT simulation results showed that the model performance based on the Nash-Sutcliffe efficiency and percent bias was acceptable for simulating three parameters; daily flow discharge, monthly sediment loads, and TP loads in the river. As a result, monthly sediment loads and TP loads increase remarkably under all future climate change scenarios except for July, when a comparable amount of precipitation is recorded during the present and future conditions. New implementation of BMPs, therefore, will be required for future climate change scenarios to achieve 50% TP load reduction in the given watershed condition. Interestingly, parallel terraces which showed good efficiency in reducing TP loads at both fields under the current weather condition cannot be effective any more under the worst-case weather scenario in the future climate. In such a case, detention ponds can be proposed as BMP alternative to parallel terraces. Overall, this study not only demonstrates that watershed management plans using BMPs should be adjusted according to climate change scenarios, but also that the hybrid use of SWAT model and AI can help in refining existing and future BMPs at affordable cost.

1. Introduction

Climate change, which is accompanied by an increase in atmospheric concentrations of greenhouse gases such as carbon dioxide and ozone (i.e., global warming), weakens security of global water resources (Vörösmarty et al., 2000). The (global) hydrologic cycle intensifies with strong climate change, which redistributed water on the planet beyond expectations of climate models based on historical weather records (Allen and Ingram, 2002). In fact, projections of different levels of future climate scenarios available from the Intergovernmental Panel on Climate Change (IPCC) to the climate models was found to show substantial increases in global-mean evaporation

* Corresponding author.
E-mail address: joonkim@gist.ac.kr (J.H. Kim).

https://doi.org/10.1016/j.ecoleng.2018.05.006
Received 7 February 2018; Received in revised form 19 April 2018; Accepted 4 May 2018
Available online 21 May 2018
0925-8574/

and precipitation on average (Labat et al., 2004; Li et al., 2013). This clearly implies that significant changes of hydrologic regimes (e.g., more rapid runoff and flooding), contaminant transport processes (e.g., increased sediment and chemical fluxes), and ecosystem functions (e.g., less abundant species and diversity) in water resources will occur under future climate conditions (O'neil et al., 2012; Peperzak, 2003). Therefore, new mitigation strategies are needed at all sectors relying heavily on water resources, even though episodes on water crisis (e.g., water shortage, contamination, and water-related disasters) differ considerably across the regions, in addition to the climate models and future scenarios (Iglesias et al., 2007; Werritty, 2002).

Best management practices (BMPs) are commonly known as an alternative management strategy to reduce nonpoint source (NPS) pollutants by controlling runoff, sediment, and nutrient losses from agricultural areas (Kaini et al., 2008; Lam et al., 2011). BMPs can be classified into structural and non-structural management practices. Structural BMPs such as pond, terraces, wetland, and filter strip are commonly applied to natural systems (Kaini et al., 2008). Non-structural BMPs, including tillage practices and control fertilizer, are institutional and educational practices designed to minimize pollutants or amount of stormwater runoff (Lam et al., 2011). The effectiveness of BMPs for controlling NPS varies depending not only on the type of crops, but also on geological and hydrological characteristics of watersheds (Maringanti et al., 2009). Thus, the performance of BMPs should be sensitive to climate change. A modeling study by Woznicki and Pouyan Nejadhashemi (2014) revealed that the performance of BMPs varied both seasonally and spatially by differing climate scenarios. Although they may not be suitable under future climate and hydrological conditions (Woznicki and Nejadhashemi, 2012), many BMPs implementation strategies recently developed have not taken climate change into account (Arabi et al., 2006; Kaini et al., 2012; Maringanti et al., 2009; Srivastava et al., 2002).

This study aims to assess how the relative effectiveness of agricultural BMPs changes with changing climates, hypothesizing that an optimal BMP in the current climate may not be optimal in warmer future climates. To explore the impacts of climate change on the performance of BMPs, we used the SWAT model. The SWAT model has been widely used for assessing the impacts of climate change on surface runoff and NPS (Githui et al., 2009; Gosain et al., 2006; Hanratty and Stefan, 1998; Jha et al., 2004). The effectiveness of implementation of BMPs removing non-point nutrient inputs from agricultural areas has been explored with the SWAT model (Bracmort et al., 2006; Gitau et al., 2008; Lee et al., 2010). However, the SWAT has been rarely used to compare the performance of various BMPs under different climates. In this study, the SWAT model was run under three different climate change scenarios (RCP 2.6, 4.5, 8.5).

Coupled with the SWAT, the Multi Objective Decision Support System (MODSS) was used to select optimal BMPs that represent the best compromise between load reduction and implementation cost (Bekele and Nicklow, 2005; Maringanti et al., 2011). We applied the SWAT and the MODSS to the Yeongsan River (YR) watershed, Korea. Dominated by agricultural areas (33%), the YS River watershed has caused eutrophication and serious algal blooms in the river (Cha et al., 2009; Cho et al., 2009). Based on the case study, optimal BMPs with respect to both load reduction and cost were selected and allocated across the watershed, and the effects of climate conditions on the effectiveness of BMPs implementation were analyzed.

2. Materials and methods

2.1. Site description

The study site is located in the upper reaches of the YR watershed in South Korea (Fig. 1). The watershed area is approximately 724 km^2 and is divided into nine sub-watersheds. The land use within the watershed primarily consists of forests (51%) and rice paddies (24%). Other land use types include soybean fields (10%), urban areas (9%), and hayfields (4%). Nonpoint source pollution, in particular from agricultural activity, has been the major source that caused the deterioration of the water quality of the Yeongsan River (Kang et al., 2010, 2009; Ki et al., 2007). The whole process from preparing input files to develop SWAT model to comparing optimal BMP implementation strategies under different climate conditions is presented in Fig. 2.

2.2. Model development

2.2.1. Description of SWAT model

The SWAT, developed by the United States Department of Agriculture, has been widely used to evaluate the impacts of agriculture activity on water quality in a watershed on a daily basis. Therefore, SWAT model can compare the performance of differing BMPs under various climate conditions at the watershed-scale (Arnold et al., 1998). SWAT model is a physical-based and continuous-time model and appropriate to simulate over long periods of stream flow, and loadings of nutrients and pesticide. The SWAT model for the YR watershed simulated daily flow discharge, monthly sediment loads and total phosphorus (TP) loads at the Mareuk (MR) station located at upstream of YS River. A watershed in a SWAT model is divided into a number of subbasins which are subdivided into hydrologic response units (HRUs), each of which is comprised of homogeneous land use, slope, and soil type (Gitau et al., 2004).

2.2.2. Data description

Topographical, land use, soil, and point source pollution data were obtained from the online water management information system (WAMIS) (http://www.wamis.go.kr). The topographical data were used to generate a stream network, a basin, and sub-basins. The land use data, obtained from the WAMIS, were used to generate 16 different land use types, including forest, agriculture, and urban areas. The soil within the watershed was classified into 164 different types. The point sources of pollution included discharge from two sewage treatment plants located in the basin. Meteorological data were acquired from the Korea Meteorological Administration (KMA) web site (http://www.kma.go.kr). The agriculture activity database was acquired from the Korea Rural Development Administration (http://www.rda.go.kr). The database included the timing of tillage operation, fertilizer application, planting/beginning of growing season, harvest and kill operation, the quantity of fertilizer applied and the method of tillage. Water quality data, acquired from the Korea water information system web site (http://water.nier.go.kr), included daily flow discharge, monthly sediment concentration, and monthly TP concentration sampled at MR station from year 2000–2010.

2.2.3. Sensitivity analysis, model calibration and validation

A sensitivity analysis on model parameters was performed based on the Latin Hypercube One-factor-At a Time (LH-OAT), a combination of the Latin hypercube (LH) sampling as an initial point and OAT design (Holvoet et al., 2005). The LH simulation, as an alternative to Monte-Carlo sampling, simultaneously selects random values over the parameter space (McKay et al., 1979). Through the sensitivity analysis significant parameters for calibrating the SWAT model were determined.

The simulation period was 11 years from 2000 to 2010, which was further divided into 3 subperiods: spin-up period (2000–2002), calibration period (2003–2006), and validation period (2007–2010). The parameters selected from the sensitivity analysis were used for calibration. The Nash-Sutcliffe efficiency coefficient (E_{NS}) (Eq. (1)) (Krause et al., 2005), and the percent bias (PBIAS) (Eq. (2)) were used for model evaluation.

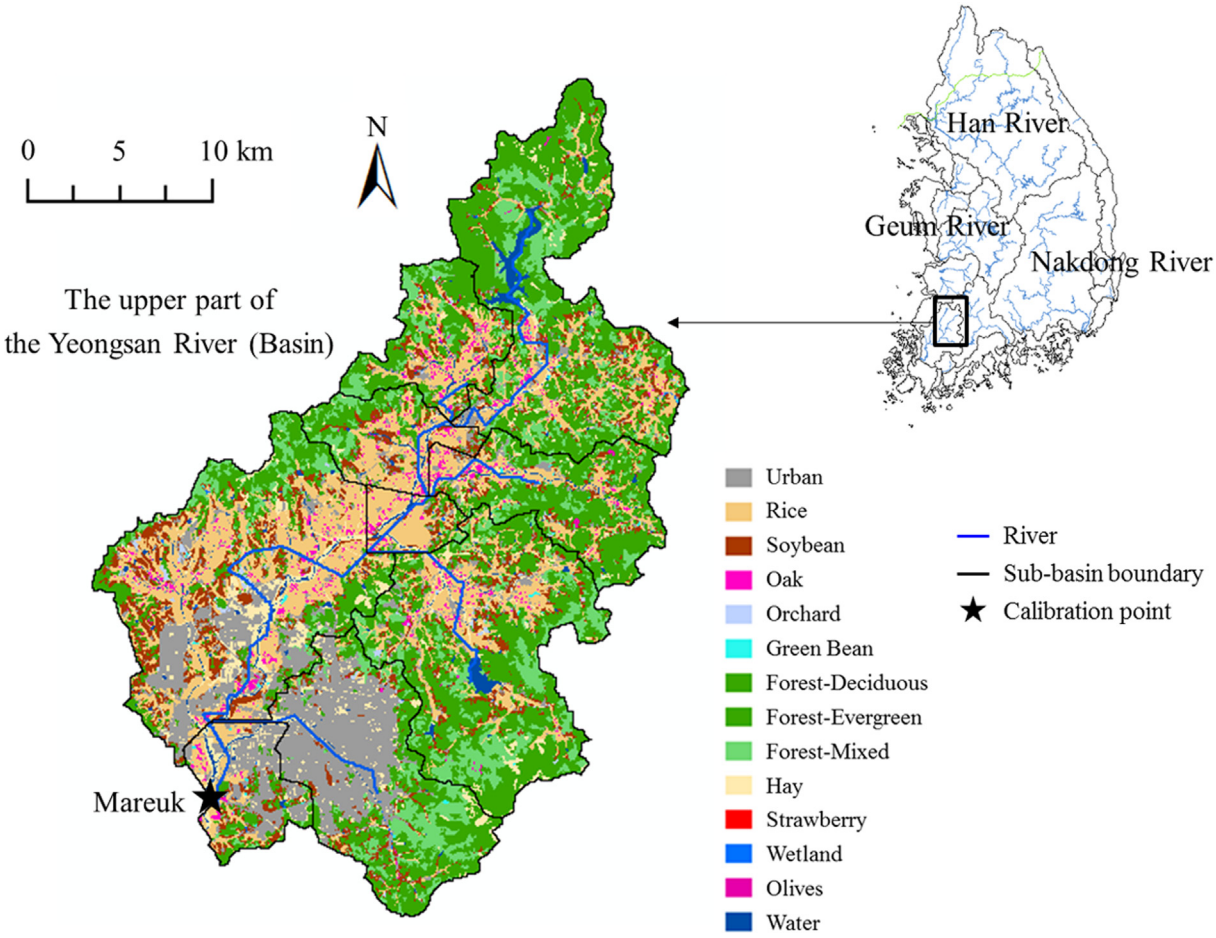

Fig. 1. The land use characteristics of the upper part of the Yeongsan River (Basin) in Korea. The upper basin area is divided into small drainage units from the sub-basin discretization process in the SWAT, where the final outlet Mareuk (MR) is used as a calibration point. Note that rice and soybean fields are selected as the target areas that are only suitable for Best Management Practices implementation in the simulation.

$$E_{NS} = 1 - \frac{\sum_{i=1}^{n} (O_i - P_i)^2}{\sum_{i=1}^{n} (O_i - O)^2} \quad (1)$$

$$PBIAS = \frac{\sum_{i=1}^{n} (O_i - P_i) * (100)}{\sum_{i=1}^{n} O_i} \quad (2)$$

where O is the observed values and P is the predicted values.

2.3. Bmps representation

The developed SWAT model was used to simulate the effects of BMPs for reducing the TP runoff from rice paddies and soybean fields. Four BMPs were applicable for rice paddies: conservation tillage (CT), parallel terrace (PT), contour cropping (CC), and detention pond (DP). In addition to these four BMPs two more BMPs were applicable for soybean fields: no tillage (NT) and riparian buffers (RB). The SWAT representation for BMPs application is presented in Table 1. Note that NT was not applicable for rice paddies because rice cultivation requires tillage practices. Also, RB was considered not applicable because the surface runoff from rice paddy field is usually concentrated into drainage channels and discharged into the river without passing the RBs. The effects of CT and NT, which reduce the amount of surface runoff, were simulated by changing the curve number (CN) and roughness coefficient (Table 1) in the SWAT. Terraces have the effect of reducing peak flow and sediment erosion on stream water quality (Artita et al., 2008). The effects of PTs were simulated by changing a CN and USLE_P values. CC is an effective method for reducing sediment and fertilizer loss by planting parallel the crops. The effects of CC were simulated with the reduced CN and adjusted USLE_P values. A DP can reduce the peak flow, sediment and nutrient loss by retaining the runoff and is simulated with changed hydraulic conductivity, the fraction of HRU draining to pond, and emergency spillway area (Kaini et al., 2012; Artita et al., 2008). Riparian zone vegetation prevents sediment and nutrients runoff draining directly into streams (Zhang and Zhang, 2011). The effects of RBs are represented by changing the edge width of field filter strip (FILTERW). Four BMPs for rice paddy field, six BMPs for soybean field, and BMPs for each crop combined to constitute a total of 31 BMP types.

The SWAT model which simulated BMPs implementation generated two response matrices for costs and TP yield estimated at an HRU scale in the watershed. The total costs and TP yields were estimated based on 97 HRUs with agricultural land uses, 39 and 59 HRUs with rice paddy and soybean fields, respectively. Detailed information on the costs of implementing BMPs was obtained from multiple sources (Table 2).

TP yield was calculated across agricultural HRUs and BMP types using the first objective function (Eq. (3)).

$$\text{TP yield}(i,j) = \sum_{i=1}^{31} \sum_{j=1}^{12} [Min_p(i,j) + Org_p(i,j)] \quad (3)$$

where i is BMP type, j is agricultural HRU, Min_p (i, j) is the mineral

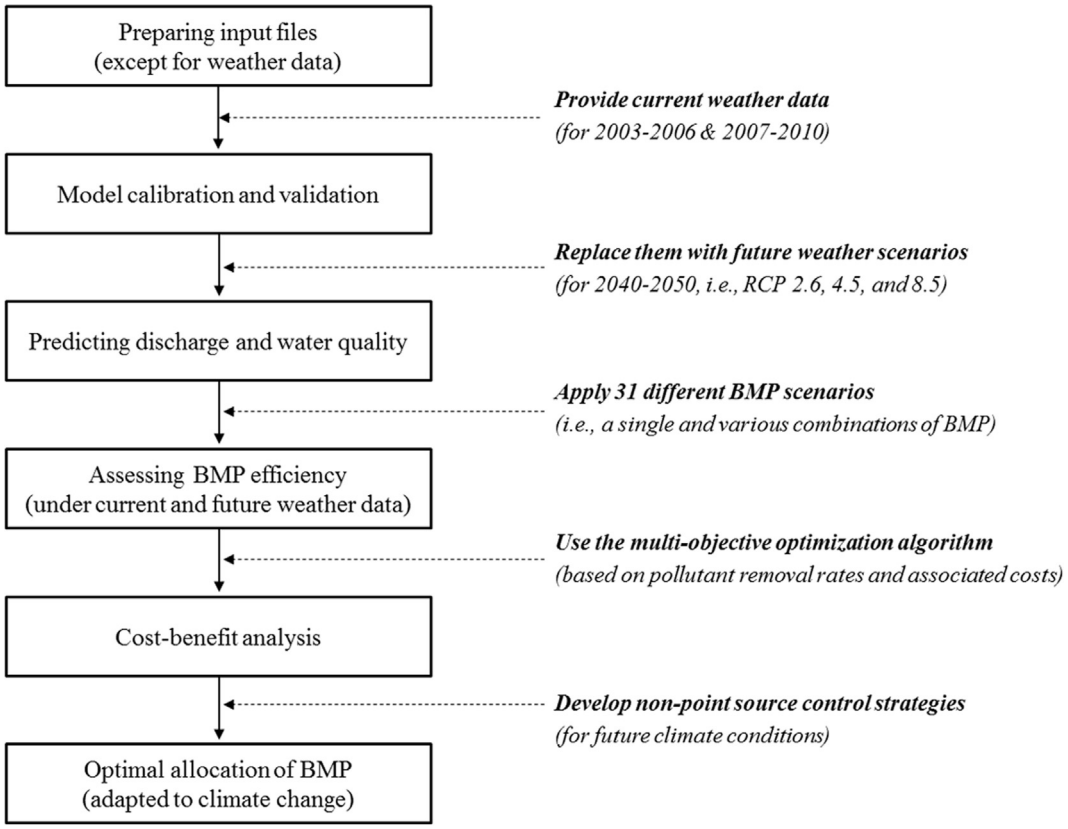

Fig. 2. A flowchart for optimal allocation of Best Management Practices (BMP) for rice and soybean fields in the study area which is best adapted to future weather scenarios of RCP 2.6, 4.5, and 8.5. Once the SWAT has been calibrated and validated with current weather data (for the period 2003–2010), different BMP implementation strategies for future weather scenarios were developed using the multi-objective optimization that simultaneously satisfied two conditions, the maximum pollutant removal and the minimum implementation cost.

phosphorus loading at j th HRU [kg ha^{-1}] when i th BMP was applied and Org_p (i, j) is the organic phosphorus loading at j th HRU [kg ha^{-1}] when i th BMP was applied.

The cost was calculated using the second objective function as follows:

$$\text{Costs}(i,j) = \sum_{i=1}^{31} \sum_{j=1}^{12} C(i) \times A(j) \quad (4)$$

where C(i) is the total unit costs for the ith BMP [\$ ha^{-1}], and A(j) is the area for the j th HRU [ha].

Table 1
Key parameters and their recommended values in each Best Management Practices (BMP) used for the SWAT simulation under current and future climate scenarios.

Types of BMP[a]	Parameters	Values[d]	Types of input files[e]	Description	Sources
CC	CN2[b]	−3	MGT	Initial SCS runoff curve number for moisture condition II	Tuppad et al. (2010)
	USLE_P[c]	0.5 or 0.6	MGT	USLE equation support practice factor	
CT	TILL_ID	3	MGT	Tillage implement code from tillage database	Ullrich and Volk (2009)
	CN2	−2	MGT	Initial SCS runoff curve number for moisture condition II	
	OV_N	0.30	HRU	Manning's "n" value for overland flow	
DP	PND_K	0	PND	Hydraulic conductivity through bottom of ponds (mm/hr)	Kaini et al. (2012)
	PND_FR	0.75	PND	Fraction of sub-basin area that drains into ponds	
	PND_ESA	0.01	PND	Surface area of ponds when filled to emergency spillway (ha)	
NT	TILL_ID	4	MGT	Tillage implement code from tillage database	Ullrich and Volk (2009)
	CN2	−2	MGT	Initial SCS runoff curve number for moisture condition II	
	OV_N	0.30	HRU	Manning's "n" value for overland flow	
PT	CN2	−5	MGT	Initial SCS runoff curve number for moisture condition II	Artita et al. (2008)
	USLE_P	0.1 or 0.12	MGT	USLE equation support practice factor	
RB	FILTERW	10	MGT	Width of edge-of-field filter strip (m)	Maringanti et al. (2011)

[a] Refer to Table 1 for explanation of BMP abbreviations.
[b] The parameter CN2 for each BMP is adjusted by adding the recommended values to the calibrated values in each HRU evenly.
[c] The low and high values are used when the slope ranges between 1 and 2% and between 3 and 8%, respectively.
[d] The recommended values of key parameters for each BMP can be different from other sources.
[e] HRU and MGT are input files related to general characteristics of HRU and management scenarios defined at the HRU level, whereas PND refers to a file that includes information on impoundments at the sub-basin level.

Table 2
Representative Best Management Practices (BMP) and their implementation costs used for the SWAT simulation under current and future climate scenarios.

Types of BMP	Description	Benefits	Unit costs ($/ha)[a]	Sources
Contour cropping (CC)	Planting crops along the contour line (i.e., across the slope) to minimize peak runoff	Peak flow reduction as well as infiltration and particle deposition enhancement	16.80	Maringanti et al. (2011)
Conservation tillage (CT)	Tillage methods that retain more than 30% of crop residues after planting to protect soil from erosion	Improvements in soil moisture status and infiltration as well as pollutant load and peak flow reduction	0	Rabotyagov et al. (2010)
Detention ponds (DP)	Basins that temporarily retain stormwater runoff for a specified period of time	Peak flow reduction as well as limited pollutant removal and bank erosion control	99.00	Kaini et al. (2012)
No tillage (NT)	Tillage methods that retain virtually 100% of crop residues undisturbed year around to promote minimal soil disruption	Improvements in soil stability and growth with pesticide and fertilizer runoff reduction	17.25	Rabotyagov et al. (2010)
Parallel terrace (PT)	Ridges and channels constructed on moderate to steep slopes to reduce peak runoff and soil erosion	Peak flow reduction, soil and wind erosion control, and limited pollutant removal	74.90	Maringanti et al. (2011)
Riparian buffers (RB)	Vegetated zones that alleviate the impacts of stormwater runoff on adjacent surface waters	Pollutant load and peak flow reduction, bank stabilization, and habitat enhancement	29.35	Maringanti et al. (2009)

[a] Unit costs for each BMP may vary considerably across data sources.

2.4. MODSS

2.4.1. Multi-objective genetic algorithms

MODSS is a decision support framework, which is technically based on the genetic algorithms (GAs). A GA is a global search technique in which the problem of selection and placement of BMPs can be decided using non-dominated sorting genetic algorithm-2 (NSGA-2) (Bekele et al., 2011). NSGA-2 is a popular multi-objective optimization algorithms developed by Deb et al. (2002). In the MODSS each of the 97 HRUs is considered as a variable for which an optimal BMP is globally searched for with the following objective functions: (1) minimizing the TP load and (2) minimizing the cost for BMPs implementation. A population of the MODSS consists of a selected BMP type in a given HRU. One BMP type (a gene) of a population is duplicated if it meets the objective functions better than the other BMP types. The other BMP types that are not duplicated are removed. The selected population goes through crossover and mutation processes to obtain a new population set of genes. The new population is evaluated through the next round of selection, crossover, and mutation processes until reaching the designated number of generation.

2.4.2. Sensitivity analysis of GAs parameters

In general, an increase in the population size and number of generations can enhance performance of GA at the expense of computation time needed to obtain an optimal solution (Maringanti et al., 2011). A sensitivity analysis of GA parameters was performed to determine the influence of these parameters on the Pareto-optimal front. The Pareto-optimal front is regarded as a best mathematical solution to a multi-criteria problem. Pareto-front changes depending on different population sizes (100, 500, 1000, 2000) and numbers of generation (1000–20,000). Exponential function (Eq. (5)) was used to find the optimal value of the number of generations. The optimal number of population seizes and generations was decided at a, b in exponential function does not change when the number of generations is increased gradually.

$$y = a^{*}\exp(-b^{*}x) \tag{5}$$

where x is TP loads (objective 1), y is total implementation costs (objective 2) and a and b are coefficients.

2.5. Assessment of climate change impacts on BMPs

The climate change scenarios used were the Korean peninsula climate change scenarios (12.5 km) from Korea meteorological administration (KMA). Three emission scenarios from the representative concentration pathway (RCP) 2.6 (420 ppm CO_2 concentration), 4.5 (540 ppm), and 8.5 (940 ppm) from the IPCC fifth assessment report were used to represent future greenhouse gas emissions. The future climate projections under the four emission scenarios were based on the ensemble of coupled general circulation model (GCM) simulations conducted in HadGEM2-AO. The regional climate model (RCM), which converts the large-scale information from GCM to small scales, consists of HadGEM3-RA with 12.5 km × 12.5 km resolution. RCMs provide future climate data, including daily precipitation, daily relative humidity, daily maximum temperature, daily minimum temperature, and daily mean wind speed, which are available until the year 2100. However, precipitation and temperature from RCM is rarely used directly for assessing hydrological impacts because they often show significant biases compared to observed climate data (Teutschbein and Seibert, 2012). Therefore, the bias correction methods were applied to correct potential deviations in the RCM-simulated precipitation and temperature data. The local intensity scaling (LOCI) and linear scaling methods were applied for precipitation and temperature bias corrections, respectively (Teutschbein and Seibert, 2012). Observed precipitation and temperature during the period 1979–2005 were used as reference conditions.

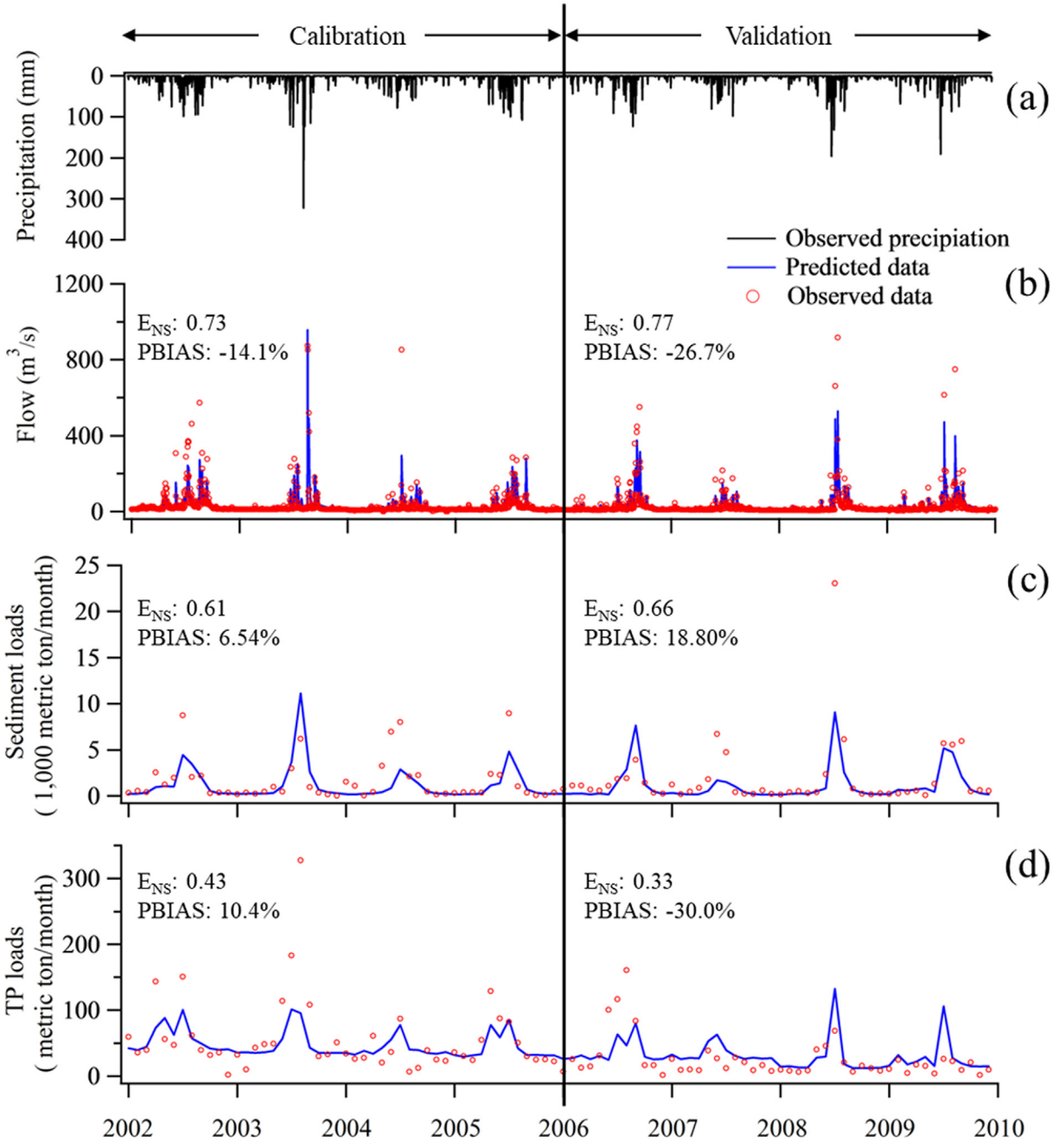

Fig. 3. Performance of the SWAT model assessed in Mareuk during calibration (for 2003–2006) and validation periods (for 2007–2010): (a) daily precipitation measurements and the observed and predicted data for (b) daily river discharge, (c) monthly sediment loads, and (d) total phosphorus (TP) loads. E_{NS} indicates the Nash-Sutcliffe coefficient.

2.5.1. Bias correction for precipitation

The LOCI, a three-step analysis, corrects bias by adjusting the mean wet-day frequencies and wet-day intensities of precipitation time series (Teutschbein and Seibert, 2012). First, a RCM-specific precipitation threshold was calibrated such that the number of RCM-simulated days exceeding this threshold matches the number of observed days with precipitation larger than 0 mm. Then, during the control period (1979–2005) and scenario period (2040–2050) the days in which the amount of precipitation was less than the threshold was redefined as 0 mm precipitation.

$$P_{contr*1}(d) = \begin{cases} 0, if\ P_{contr}(d) < P_{th,contr} \\ P_c^{ntr}(d), otherwise \end{cases} \quad (6)$$

$$P_{scen*1}(d) = \begin{cases} 0, if\ P_{scen}(d) < P_{th,contr} \\ P_{scen}(d), otherwise \end{cases} \quad (7)$$

where $P_{contr}(d)$ is daily precipitation of RCM-simulated during 1979–2005, $P_{contr*1}$(d) is bias corrected daily precipitation of RCM-simulated during 1979–2005 in the first step, $P_{th.contr}$ is an RCM-specific precipitation threshold, $P_{scen}(d)$ is daily precipitation of RCM-simulated during 2040–2050, and $P_{scen*1}(d)$ is bias corrected daily precipitation of RCM-simulated during 2040–2050 in the first step.

In the second step, a linear scaling factor s was calculated from the monthly mean wet-day intensities.

$$s = \frac{\mu_m(P_{obs}(d)|P_{obs}(d) > 0mm)}{\mu_m(P_{contr}(d)|P_{contr}(d) > P_{th,contr}) - P_{th,contr}} \quad (8)$$

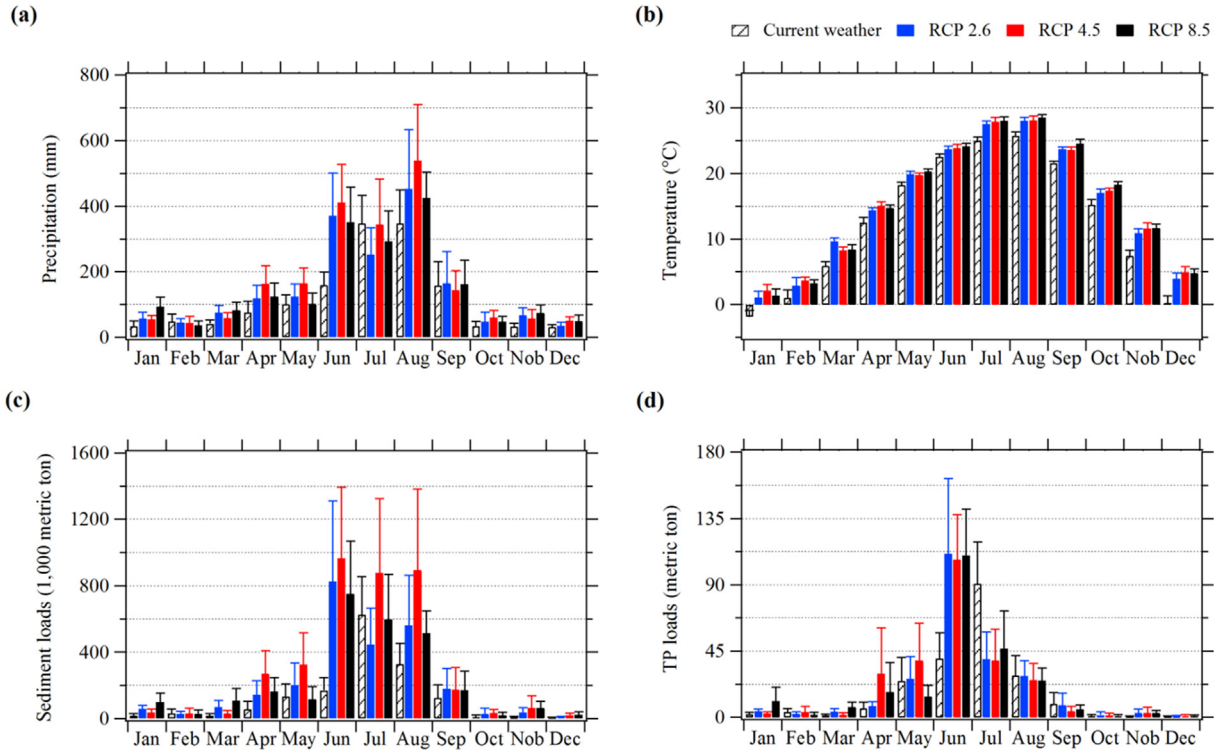

Fig. 4. Comparison of different weather inputs and their resulting outputs in the SWAT: monthly averaged (a) precipitation, (b) temperature, (c) sediment loads, and (d) total phosphorus (TP) loads. The simulation was performed during the periods 2000–2010 (for current weather condition including the initial warm-up period 2000–2002) and 2040–2050 (for future weather scenarios of RCP 2.6, 4.5, and 8.5). Error bar represents the 95% confidence interval.

where P_{obs} *(d)* is observed daily precipitation during 1979–2005, μm is mean within monthly interval, and s is scaling factor.

Finally, the precipitation of control period and scenario period was corrected by

$$P_{contr*}(d) = P_{contr*1}(d)*s \quad (9)$$

$$P_{scen*}(d) = P_{scen*1}(d)*s \quad (10)$$

where P_{contr*}*(d)* is final bias-corrected daily precipitation of RCM-simulated 1979–2005 and P_{scen*}*(d)* is final bias-corrected daily precipitation of RCM-simulated 2040–2050.

2.5.2. Bias correction for temperature

The RCM-simulated temperature was calibrated by using the linear scaling approach (Leander and Buishand, 2007). Linear scaling operates (Eq. (11)) with yearly correction values based on differences between observed and RMC-simulated data.

$$T_{RCM*} = T_{RCM} + (T_{mean.his} - T_{RCM.his}) \quad (11)$$

where $T_{mean.his}$ is observed yearly mean temperature during 1979–2005, $T_{RCM.his}$ is RCM-simulated yearly mean temperature during 1979–2005, T_{RCM} is RCM-simulated daily temperature during 2040–2050, and T_{RCM*} is bias-corrected daily temperature of RCM-simulated 2040–2050.

2.5.3. Application of climate change scenarios in SWAT model

We selected three future climate scenarios (RCP 2.6, 4.5, and 8.5) to project future (years 2040–2050) climate conditions. Future precipitation and temperature projections were used to estimate flow discharge, sediment load, TP load, and BMP allocation for the years 2040–2050 using SWAT. To assess the impacts of climate change on temporal TP load patterns and composition of optimized BMPs, projected TP loads and BMPs were compared with those in the present climate represented by the years 2000–2010.

3. Results and discussion

3.1. SWAT model performance

The performance of the SWAT model was assessed in terms of monthly sediment and TP levels as well as daily stream discharge at the final outlet of the YS watershed, MR (Fig. 3). The performance assessment tasks were conducted during two simulation periods, one from 2003 to 2006 (for calibration phase), and the other from 2007 to 2010 (for validation phase). Note, however, that data availability which differs by the authorizing agency prohibits the use of the identical time steps in this performance assessment. Before starting the performance assessment, all parameters required for accurate simulation of sediment and TP concentrations as well as stream discharge was initially selected using the LH-OAT method, one of universal sensitivity analysis methods. The major parameters that significantly affected stream discharge were the surface runoff lag coefficient (named as the subroutine SURLAG in SWAT), the baseflow alpha factor (ALPHA_BF), the Manning's roughness coefficient for channel flow (CH_N(2)), the effective hydraulic conductivity in main channel alluvium (CH_K(2)), and the initial Soil Conservation Service (SCS) runoff curve number (CN) for moisture condition II (CN2). Sediment concentrations were mostly sensitive to the peak rate adjustment factor (PFR), the exponent in sediment transport (SPEXP), the coefficient in sediment transport equation (SPCON), and the others. Seven parameters were large enough to provide sufficient prediction accuracy for TP concentrations; algal respiration rate at 20 °C (RHOQ), biological mixing efficiency (BIOMIX), phosphorus enrichment ration (ERORGP), and the others. Collectively, a total of twelve, five, and seven parameters needed to be adjusted among twenty-seven flow-, twelve sediment-, and fourteen TP-related parameters, respectively. Note that the remaining parameters except for those were fixed at default values (Table S1).

The selected parameters were calibrated both manually (for stream discharge) and automatically (for sediment and TP levels). Specifically,

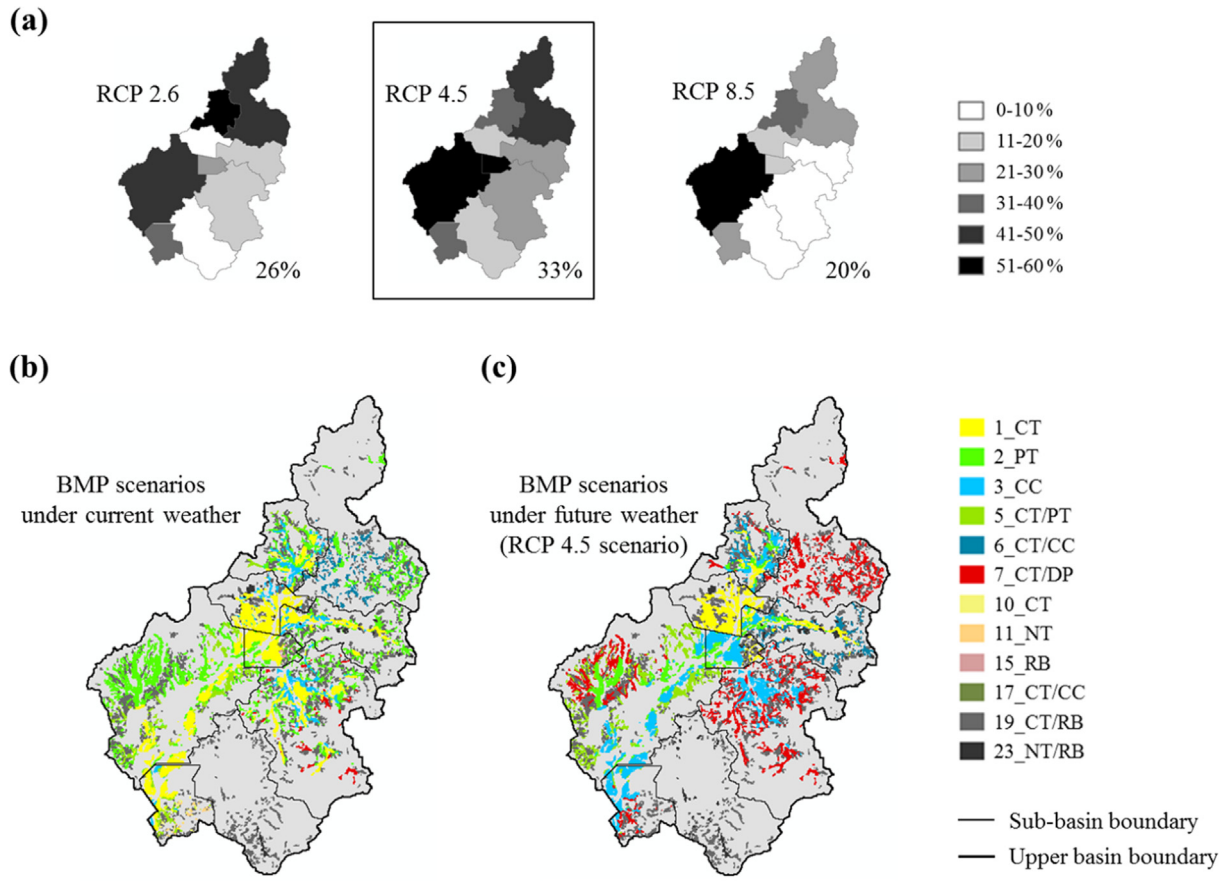

Fig. 5. Optimal Best Management Practices (BMP) implementation strategies for the study area with 50% reduction of total phosphorus (TP) load under present and future climate scenarios of RCP 2.6, 4.5, and 8.5: (a) depicts the amount of change in the types of BMP assigned for individual sub-basins between current and any of these future weather scenarios (see a gray scale or an absolute value of the percent difference): (b) and (c) present two examples of the proposed allocation of BMP to reduce the TP loads under current and the RCP 4.5 scenario, respectively.

a pattern search algorithm was used for automatic calibration process. Fig. 3b through d illustrate time series plots of sediment and TP concentrations as well as stream discharge predicted after manual and automatic calibration of those parameters in the model. The prediction accuracy was assessed with respect to E_{NS} and PBIAS, which were recommended as the best indicators in the user community (Moriasi et al., 2007). From Fig. 3b, it was shown that the observed stream discharge was in fairly good agreement with the predicted one during both the calibration and validation periods, in terms of magnitude and pattern. However, there were also some exceptions showing a large deviation between the observed and predicted values during the rainy season, which needed to be further clarified by investigation on input from other water sources in the following study. The values of E_{NS} and PBIAS estimated were 0.73 and −14.1% for the calibration period and 0.77 and -26.7% for the validation period. The model also provided a good fit to the monthly observation of sediment and TP load which were calculated using daily flow discharge and monthly water quality concentrations excluding several outliers that were coincided with heavy rainfall events (see Fig. 3c and d). However, the TP concentrations still appeared to be overestimated slightly in the non-rainfall seasons, requiring a more detailed study for particular sink terms which removed or lowered the TP concentrations in the river channel. In terms of sediment concentrations, the values of E_{NS} and PBIAS for the calibration period were calculated to be 0.48 and 6.54% and those of the validation period corresponded to 0.67 and 18.8%. Similarly, the values of E_{NS} and PBIAS in predicting TP concentrations were computed to be 0.56 and 0.39, 10.4% and −30.0% for the calibration and validation phases, respectively. In summary, the model was found to show acceptable accuracy for describing the fate and transport of target pollutants (i.e., sediments and TP) in the YS watershed, along with stream discharge which show the best prediction performance among them.

3.2. Effects of climate change on TP loads

After fine-tuning the SWAT model for the YS watershed, the current weather data were replaced with the new weather scenarios to quantify the relative change in contaminant loads. Fig. 4 illustrates different sets of example weather inputs (i.e., precipitation and temperature under the current and future scenarios) and their corresponding outputs (i.e., sediment and TP loads) which are provided to and received from the find-tuned model, respectively. In the figure, RCP scenarios 2.6 (the lowest level of greenhouse gas emission), 4.5 (the intermediate level), and 8.5 (the highest level) represent the future weather data projected to the YS watershed for the period 2040–2050. In contrast, the current weather data cover the period from 2000 to 2010 that combines the calibration and validation phases. We believe that the inclusion of this scenario will make our analysis more complicated than needed because future climate scenarios was clearly different in an aspect of rainfall pattern in summer season compared with current climate condition. From Fig. 4a and b, precipitation and temperature showed clear seasonal patterns with high peaks at the wet summer season (June to August) and low peaks at the dry winter season (December to February), regardless of whether scenarios, which was well-accorded with the East Asian monsoon system. The average values for both precipitation and temperature in all future weather scenarios were generally higher than those of the current scenario, with a few exceptions for precipitation in February, July, and September. Out of the scenarios, RCP 4.5 appeared to result in a remarkable increase in precipitation for

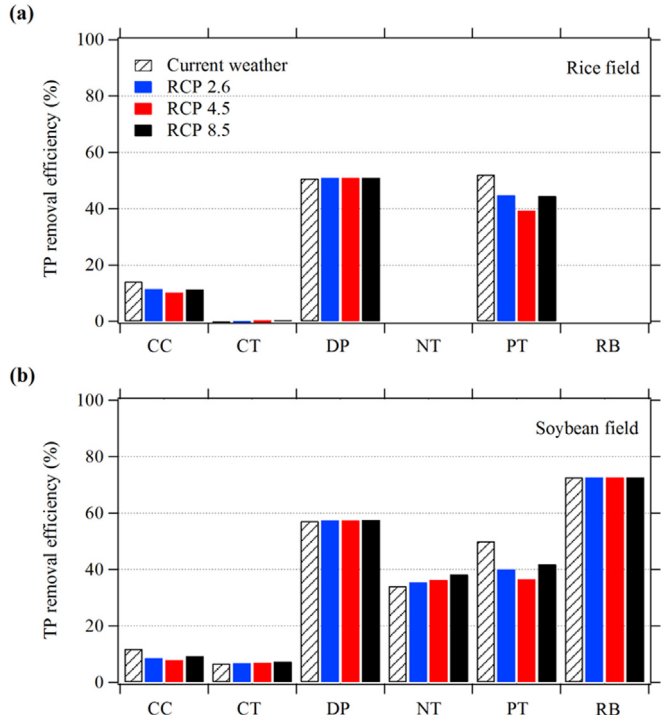

Fig. 6. Comparison of total phosphorus (TP) removal efficiencies among different Best Management Practices (BMP) which are implementable in (a) rice and (b) soybean fields for the study area. The TP removal efficiencies of each BMP represent the gross sum which is aggregated over the periods 2000–2010 (for current weather condition including the initial warm-up period 2000–2002) and 2040–2050 (for future weather scenarios of RCP 2.6, 4.5, and 8.5). Refer to Table 1 for explanation of BMP abbreviations.

several months (e.g., June and August) in the YS watershed, whereas temperature changes were most pronounced in RCP 8.5 according to the emissions levels. The altered precipitation and temperature regimes caused substantial changes in sediment and TP yields over the YS watershed (see Fig. 4c and d). The altered precipitation and temperature appeared to have a bigger or a more direct influence on sediment load than TP load due to complex mechanisms involved in the phosphorus cycle processes (compare their yields between July and August). The most significant increase in sediment load was observed for RCP 4.5, whereas sediment yields resulted from the other two scenarios were quite comparable with each other. Interestingly, TP load in June was higher for all future weather scenarios than that of the current scenario although no apparent pattern was noticed in the remaining months. The remarkable increase of sediment yield caused by the increase of precipitation in June and timing of fertilizer application in May seemed to be partially responsible for this abrupt increase of TP load (in June) under the new weather scenarios, as compared to those of other months (Cho, 2003; Lee et al., 2006). Bulut and Aksoy (2008) also verified a strong positive relationship between the P loads and the fertilizer application rates. This result also reflected that TP load should be carefully estimated by the fine-tuned model with a good representation of the observed parameter rather than a simple function of a series of weather inputs. To recap briefly, although previous studies suggested a strong relationship between sediment and TP yield rates as well as between peak TP yields and rates (or timing) of fertilizer application, those effects appeared to diminish under the new weather scenarios (Mockus, 1972). In other words, sediment and TP yields considerably varied from scenario to scenario.

3.3. Effects of climate change on BMPs implementation

It may be very important to reduce TP loads to the river when the impact of climate change on TP loss has become obvious in the watershed. MODSS determined the optimized BMPs based on single and combined BMP types, using two criteria such as TP removal efficiency and cost of BMPs. The MODSS results presented that the composition of optimized BMPs changed in response to future climate change scenarios (see Fig. 5(a)). Population size and generation number used as the two parameters of the GA, were optimized at 1000 and 14,000, respectively, where the Pareto-front converged. The Pareto-optimal fronts were not distinctly different among climate change scenarios. Fig. S1 shows the result of the Pareto-optimal fronts under present climate, RCP 2.6 scenario, RCP 4.5 scenario, and RCP 8.5 scenario. Under current climate, BMP implementation costs ranging $ 0.06–3.21 million corresponded to 54.9–220 TP metric tons (i.e., 3.40–76.0% reduction) per year. Under the RCP 4.5 scenario, the cost ranged $ 0.12–3.34 million that corresponded to 77.3–269 TP metric tons (i.e., 4.50–72.5% reduction) per year. TP load reductions by 50% corresponded to 114 and 142 TP loads (metric tons/yr) and $1.00 million and $1.23 million under current climatic conditions and the RCP 4.5, respectively.

Fig. 5(a) presents the percent changes in the optimized BMP composition for each sub-watershed depending on different climate change scenarios. The percent changes were calculated by comparing each optimized BMP composition under the future climate scenarios to the optimized BMP composition under the current climate. The largest percent changes in the optimized BMP composition were predicted from the RCP 4.5. The optimized BMPs under the RCP 4.5 were changed by 33% on average across the watershed, whereas less than 30% changes were predicted from the other scenarios (Fig. 5(a)).

A clear distinction of the proposed BMPs in the watershed under current climate and the RCP 4.5 was introduced in Fig. 5(b) and (c). Fig. S2 (See Supplementary information) shows the proposed allocation of

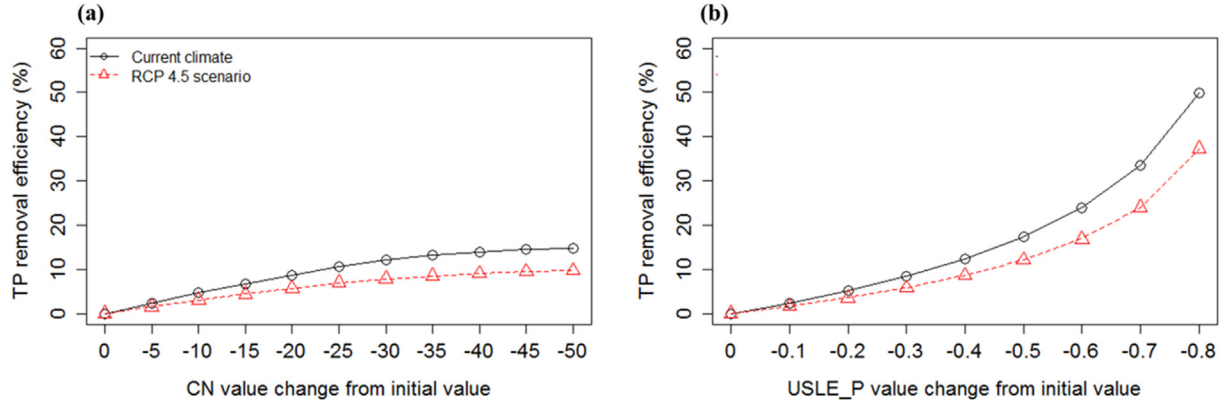

Fig. 7. Sensitivity of the SWAT model to two important parameters of simulating the performance of BMPs: (a) runoff curve number for moisture condition (CN) and (b) USLE equation support practice factor (USLE_P) value.

BMP under RCP 2.6 and RCP 8.5. The MODSS allocated an optimized BMP type for each of 97 HRUs. Among the total 31 BMPs, 12 BMP types and 8 BMP types were selected for the current climate and the RCP 4.5, respectively. Under the current climate, BMPs predominantly included CT (38%), PT (28%), and CC (18%) for rice paddy fields and CT/RB (83%) for soybean fields (Fig. 5(b)). On the other hand, BMPs under the RCP 4.5 predominantly included CC (30%), CT (23%), and CT/DP (23%) for rice paddy fields and CT/RB (86%) for soybean fields (Fig. 5(c)). CT was most frequently selected as an optimized BMP for rice paddy fields under the current climate, CT replaced with CC under the RCP 4.5. The second BMP was PT for rice paddy fields under the current climate, but PT replaced with CT/DP under the RCP 4.5. CT/RB was a prevalent BMP type allocated to soybean fields. RB in soybean fields has the benefit of less expensive costs and high TP removal efficiency as compared to PT and DP, regardless of climate conditions (Fig. 6(b)).

The TP removal efficiency of single BMP type was assessed at nine for rice paddies and 22 for soybean fields, by comparing the current climate and the future climate (Fig. 6). The results showed that TP removal efficiency was different in terms of BMP type, climate condition, and crop type. The TP removal efficiency of CT for both rice and soybean field areas did not differ much between current and future climate conditions (Fig. 6). CT had little effect in reducing TP loads from rice paddy fields (Fig. 6(a)) because there was no distinct difference between existing tillage practices and CT. In case of CT at soybean fields, TP removal efficiency showed 7% because mixing efficiency of CT has halved compared with existing tillage practice. NT and RB at soybean fields showed high TP removal efficiency of 34% and 72%, both of which did not differ much between the current climate and future climate scenarios (Fig. 6(b)).

To explain the climate effects on the TP removal efficiency of CC, sensitivity analysis for CN and USLE_P parameters, which represent the implementation of CC, was conducted (Fig. 7). TP removal efficiency increased as both CN and USLE_P values decreased and the TP removal efficiency was better for the current climate than for the RCP 4.5 when CN and USLE_P values changed in the same degree (Fig. 7). Thus, for the CN value set at −3 from initial value and USLE_P value set at either 0.5 or 0.6 depending on land slope, CC had higher TP removal efficiency in current climate (14%) than future climate conditions (11%) (Fig. 7). In addition, the efficiency difference between different crop types was observed (Fig. 6). TP removal efficiency of CC is 2% higher in rice paddy fields than soybean fields in both the current climate and the RCP 4.5 because rice is planted mainly in areas that have gentle slopes.

PT showed the largest differences in TP removal efficiency between the current climate and the future climate (Fig. 6). The PT effect on TP removal efficiency was similar to that of CC. Based on simulations using CN value of −5 and USLE_P of either 0.10 or 0.12 depending on land slope, the TP removal efficiency of PT was higher in current climate (52%) than the RCP 4.5 (39%), showing little difference between crop types (Fig. 6). While the removal efficiency of PT was higher under the current climate than under all future climate scenarios, the removal efficiency of DP was almost same between the current climate and the RCP 4.5 (Fig. 6). Accordingly, the removal efficiency characteristics of PT and DP made the largest contribution to changes in the optimized BMP composition in response to climate change.

4. Conclusion

This study evaluated the impact of climate change on the spatial allocation of BMPs in the YR watershed when reducing TP load. The SWAT model was used not only to simulate water quantity and quality in the watershed, but also to assess response of TP loads to diverse BMPs (i.e., CT, NT, PT, CC, DP, RB, or their combinations) under the current climate (for the period 2000–2010) and future climate (for the period 2040–2050). MODSS, a genetic algorithm to identify a series of the best solutions, was also employed to locate cost-effective BMPs at the HRU level. The following are the main outcomes drawn from this study.

- The SWAT model was effective in predicting the discharge and accompanying pollutant concentration profiles of the YS River on a monthly basis. The simulated and observed data matched each other fairly well during the calibration and validation periods. The optimized parameter values were within the range of recommended values, allowing us to assess the effect of individual BMPs or their combinations on TP loads to the YS river under the future climate scenarios.
- Three climate change scenarios (RCP 2.6, 4.5, and 8.5) developed from the IPCC database showed higher precipitation and temperature than current conditions in the YS watershed. Monthly sediment and TP loads of the YS river were found to be generally associated with precipitation intensity. However, TP loads appeared to be strongly affected by the timing of fertilizer application (i.e., in May every year). Sediment and TP loads were substantially higher when the RCP 4.5 among climate change scenarios was applied to the model.
- As compared to current weather condition, cost-effective BMPs allocated at the HRU level based on the MODSS algorithm varied with climate change scenarios. RCP 4.5 which showed the largest increase in sediment and TP loads among the future climate scenarios resulted in the biggest change in the allocation of BMPs at the 50% TP reduction. The performance of BMPs were highly dependent on land use patterns, so we recommended a detailed analysis on selecting BMPs or their combinations in response to watershed characteristics such as climate and land use patterns along with the target pollutants. Further study of how the potential BMP options are altered by these factors under extreme weather events is warranted.

Acknowledgements

This research was supported by a grant (Code # 413-111-005) from Eco Innovation Project funded by Ministry of Environment of Korea government.

Appendix A. Supplementary data

Supplementary data associated with this article can be found, in the online version, at http://dx.doi.org/10.1016/j.ecoleng.2018.05.006.

References

Allen, M.R., Ingram, W.J., 2002. Constraints on future changes in climate and the hydrologic cycle. Nature 419, 224–232.
Arabi, M., Govindaraju, R.S., Hantush, M.M., 2006. Cost-effective allocation of watershed management practices using a genetic algorithm. Water Resour. Res. 42, 10.
Arnold, J.G., Srinivasan, R., Muttiah, R.S., Williams, J.R., 1998. Large area hydrologic modeling and assessment part I: model development1. JAWRA J. Am. Water Resourc. Assoc. 34, 73–89.
Artita, K., Kaini, P., Nicklow, J., 2008. Generating alternative watershed-scale BMP designs with evolutionary algorithms. World Environ. Water Resourc. Congr. 2008, 1–9.
Bekele, E.G., Demissie, M., Lian, Y., 2011. Optimizing the placement of best management practices (BMPs) in agriculturally-dominated watersheds in Illinois. In: World Environmental and Water Resources Congress 2011. Bearing Knowledge for Sustainability, pp. 2890–2900.
Bekele, E.G., Nicklow, J.W., 2005. Multiobjective management of ecosystem services by integrative watershed modeling and evolutionary algorithms. Water Resour. Res. 41, 10.
Bracmort, K., Arabi, M., Frankenberger, J., Engel, B., Arnold, J., 2006. Modeling long-term water quality impact of structural BMPs. Trans. ASAE. 49, 367–374.
Bulut, E., Aksoy, A., 2008. Impact of fertilizer usage on phosphorus loads to Lake Uluabat. Desalination 226, 289–297.
Cha, S., Ki, S., Cho, K., Choi, H., Kim, J., 2009. Effect of environmental flow management on river water quality: a case study at Yeongsan River, Korea. Water Sci. Technol. 59, 2437–2446.
Cho, J.-Y., 2003. Seasonal runoff estimation of N and P in a paddy field of central Korea. Nutr. Cycl. Agroecosyst. 65, 43–52.

Cho, K., Park, Y., Kang, J., Ki, S., Cha, S., Lee, S., Kim, J., 2009. Interpretation of seasonal water quality variation in the Yeongsan Reservoir, Korea using multivariate statistical analyses. Water Sci. Technol. 59, 22219–22226.
Deb, K., Pratap, A., Agarwal, S., Meyarivan, T., 2002. A fast and elitist multiobjective genetic algorithm: NSGA-II. Evolutionary Computation. IEEE Trans. 6, 182–197.
Gitau, M., Gburek, W., Bishop, P., 2008. Use of the SWAT model to quantify water quality effects of agricultural BMPs at the farm-scale level. Trans ASABE. 51, 1925–1936.
Gitau, M., Veith, T., Gburek, W., 2004. Farm-level optimization of BMP placement for cost-effective pollution reduction. Trans. ASAE 47, 1923–1931.
Githui, F., Gitau, W., Mutua, F., Bauwens, W., 2009. Climate change impact on SWAT simulated streamflow in western Kenya. Int. J. Climatol. 29, 1823–1834.
Gosain, A., Rao, S., Basuray, D., 2006. Climate change impact assessment on hydrology of Indian river basins. Curr. Sci. 90, 346–353.
Hanratty, M.P., Stefan, H.G., 1998. Simulating climate change effects in a Minnesota agricultural watershed. J. Environ. Qual. 27, 1524–1532.
Holvoet, K., van Griensven, A., Seuntjens, P., Vanrolleghem, P., 2005. Sensitivity analysis for hydrology and pesticide supply towards the river in SWAT. Phys. Chem. Earth, Parts A/B/C 30, 518–526.
Iglesias, A., Garrote, L., Flores, F., Moneo, M., 2007. Challenges to manage the risk of water scarcity and climate change in the Mediterranean. Water Resour. Manage. 21, 775–788.
Jha, M., Pan, Z., Takle, E.S., Gu, R., 2004. Impacts of climate change on streamflow in the Upper Mississippi River Basin: a regional climate model perspective. J. Geophys. Res.: Atmospheres. 109, D9.
Kaini, P., Artita, K., Nicklow, J., 2008. Designing BMPs at a watershed scale using SWAT and a genetic algorithm. World Environmental and Water Resources Congress. Ahupua'A 2008, 1–10.
Kaini, P., Artita, K., Nicklow, J.W., 2012. Optimizing structural best management practices using SWAT and genetic algorithm to improve water quality goals. Water Resourc. Manage. 26, 1827–1845.
Kang, J.-H., Lee, S.W., Cho, K.H., Ki, S.J., Cha, S.M., Kim, J.H., 2010. Linking land-use type and stream water quality using spatial data of fecal indicator bacteria and heavy metals in the Yeongsan river basin. Water Res. 44, 4143–4157.
Kang, J.-H., Lee, Y.S., Ki, S.J., Lee, Y.G., Cha, S.M., Cho, K.H., Kim, J.H., 2009. Characteristics of wet and dry weather heavy metal discharges in the Yeongsan Watershed, Korea. Sci. Total Environ. 407, 3482–3493.
Ki, S., Lee, Y., Kim, S., Kim, J., 2007. Spatial and temporal pollutant budget analyses toward the total maximum daily loads management for the Yeongsan watershed in Korea. Water Sci. Technol. 55, 367–374.
Krause, P., Boyle, D., Bäse, F., 2005. Comparison of different efficiency criteria for hydrological model assessment. Adv. Geosci. 5, 89–97.
Labat, D., Goddéris, Y., Probst, J.L., Guyot, J.L., 2004. Evidence for global runoff increase related to climate warming. Adv. Water Resour. 27, 631–642.
Lam, Q., Schmalz, B., Fohrer, N., 2011. The impact of agricultural Best Management Practices on water quality in a North German lowland catchment. Environ. Monit. Assessment. 183, 351–379.
Lee, H., Ha, H.S., Lee, C.H., Lee, Y.B., Kim, P.J., 2006. Fly ash effect on improving soil properties and rice productivity in Korean paddy soils. Bioresour. Technol. 97, 1490–1497.
Lee, M., Park, G., Park, M., Park, J., Lee, J., Kim, S., 2010. Evaluation of non-point source pollution reduction by applying Best Management Practices using a SWAT model and QuickBird high resolution satellite imagery. J. Environ. Sci. 22, 826–833.
Maringanti, C., Chaubey, I., Arabi, M., Engel, B., 2011. Application of a multi-objective optimization method to provide least cost alternatives for NPS pollution control. Environ. Manage. 48, 448–461.
Maringanti, C., Chaubey, I., Popp, J., 2009. Development of a multiobjective optimization tool for the selection and placement of best management practices for nonpoint source pollution control. Water Resourc. Res. 45, 6.
McKay, M.D., Beckman, R.J., Conover, W.J., 1979. Comparison of three methods for selecting values of input variables in the analysis of output from a computer code. Technometrics 21, 239–245.
Mockus, V.I.C.T.O.R., 1972. National Engineering Handbook Section 4. Hydrology, NTIS.
Moriasi, D.N., Arnold, J.G., Van Liew, M.W., Bingner, R.L., Harmel, R.D., Veith, T.L., 2007. Model evaluation guidelines for systematic quantification of accuracy in watershed simulations. Trans. ASABE 50 (3), 885–900.
Leander, R., Buishand, T.A., 2007. Resampling of regional climate model output for the simulation of extreme river flows. J. Hydrol. 332, 487–496.
Li, F., Zhang, Y., Xu, Z., Teng, J., Liu, C., Liu, W., Mpelasoka, F., 2013. The impact of climate change on runoff in the southeastern Tibetan Plateau. J. Hydrol. 505, 188–201.
O'neil, J., Davis, T.W., Burford, M.A., Gobler, C., 2012. The rise of harmful cyanobacteria blooms: the potential roles of eutrophication and climate change. Harmful Algae. 14, 313–334.
Peperzak, L., 2003. Climate change and harmful algal blooms in the North Sea. Acta Oecologica. 24, S139–S144.
Rabotyagov, S.S., Jha, M., Campbell, T.D., 2010. Nonpoint-source pollution reduction for an iowa watershed: an application of evolutionary algorithms. Can. J. Agric. Econ./Revue canadienne d'agroeconomie. 58, 411–431.
Srivastava, P., Hamlett, J., Robillard, P., Day, R., 2002. Watershed optimization of best management practices using AnnAGNPS and a genetic algorithm. Water Resour. Res. 38, 3.
Teutschbein, C., Seibert, J., 2012. Bias correction of regional climate model simulations for hydrological climate-change impact studies: review and evaluation of different methods. J. Hydrol. 456, 12–29.
Tuppad, P., Kannan, N., Srinivasan, R., Rossi, C.G., Arnold, J.G., 2010. Simulation of agricultural management alternatives for watershed protection. Water Resourc. Manage. 24, 3115–3144.
Ullrich, A., Volk, M., 2009. Application of the Soil and Water Assessment Tool (SWAT) to predict the impact of alternative management practices on water quality and quantity. Agric. Water Manage. 96, 1207–1217.
Vörösmarty, C.J., Green, P., Salisbury, J., Lammers, R.B., 2000. Global water resources: vulnerability from climate change and population growth. Science 289, 284–288.
Werritty, A., 2002. Living with uncertainty: climate change, river flows and water resource management in Scotland. Sci. Total Environ. 294, 29–40.
Woznicki, S.A., Nejadhashemi, A.P., 2012. Sensitivity analysis of best management practices under climate change Scenarios1. JAWRA J. Am. Water Resourc. Assoc. 48, 90–112.
Woznicki, S.A., Pouyan Nejadhashemi, A., 2014. Assessing uncertainty in best management practice effectiveness under future climate scenarios. Hydrol. Process. 28, 2550–2566.
Zhang, X., Zhang, M., 2011. Modeling effectiveness of agricultural BMPs to reduce sediment load and organophosphate pesticides in surface runoff. Sci. Total Environ. 409, 1949–1958.